Experimental Studies on Internal Pressure and Debris Strike for Improved Tornado Induced Loads of Low-Rise Buildings

by

Partha P Sarkar[1] and Hitomitsu Kikitsu[2]

ABSTRACT

This paper presents the results of experimental studies on transient wind loads on a low-rise building induced by a tornado. The ISU Tornado Simulator at Iowa State University was used for these experiments. The internal pressure and risk of wind-borne debris strike was considered for improved prediction of these dynamic wind loads. It is shown that the magnitude of internal pressure determines the total wind uplift force on the roof and that its characteristics depend on the extent of natural leakage in the building walls as well as location of dominant openings on any of these walls. Further, the laboratory experiments show that the risk of wind-borne debris strike in a tornado increases with decreasing distance between potential wind-borne debris and target building and the characteristic of this risk depends on whether the potential debris is located within or outside the region defined by a distance of one tornado-core radius from the target building.

KEYWORDS: Tornado, Tornado simulator, Wind loads, Internal-pressure, Wind-borne debris

1.0 INTRODUCTION

Tornadoes produce rotating winds with updraft and downdraft and radial flows that intensify significantly near the ground. In most commonly occurring tornadoes that are EF-2 or of less intensity on the newly implemented Enhanced Fujita Scale, winds could reach 60 m/s (135 mph, 3-sec gust) near the ground. As a result of passage of a tornado directly over a building, transient loads are produced that peaks when the center of the tornado is within one core radius, where maximum tangential wind speed occurs, from the center of the building (Sengupta et al., 2008). In this study, only external surface pressures were measured to evaluate the loads on a low-rise cubic building. The importance of internal pressure inside a building in modifying the resultant uplift force on the roof of the building was recognized in this study but not explored because of some limitations in the model. It is known that the internal pressure inside a building is a function of air leakages through the building envelope because of intrinsic porosity that is present in the envelope and any dominant opening that could be triggered by a puncture in the envelope by wind-borne debris. This paper studies the role of internal pressure in producing the resultant wind loads in a tornado-like vortex as a function of porosity and dominant opening in a building envelope and attempts to find the strike probabilities of wind-borne debris that could create these dominant openings as a function of their relative location to the building. This work will improve the predictions of wind loads on low-rise buildings in a tornado and contribute to a probability-based design framework.

2.0 ISU TORNADO SIMULATOR PARAMETERS USED

Laboratory experiments in this study were carried out using the ISU tornado simulator at Iowa State University (ISU). Figure 1 illustrates the concept of the simulator with a schematic diagram. The details of this facility are given in Haan, et al. (2008). In these experiments, the translation speed of the tornado was fixed at 0.15m/s. The other tornado simulator parameters such as fan speed, vane angle and floor height were the same as those of “Vane 5” test case in the study by Haan, et al. (2008). A tornado-like vortex with a swirl ratio of 1.14 and radius of the tornado core of 0.53 m, where the maximum tangential velocity (= 9.7 m/s in this case) occurs, was obtained by fixing these parameters.

3.0 EVALUATION OF WIND FORCE CHARACTERISTICS

3.1 Pressure Model Details

Tornado-induced surface pressures were measured on a low-rise building model with 152.4mm by 97.5mm (6.0in. by 3.8in.) in plan dimensions and an eave height of 48.8mm (1.92in.). The shallow roof angle of the model was 1/12 (4.76^o) with the roof ridge parallel to the longer dimension. The configuration of this model is the same as that used in the study by Oh et al. (2007). The model was made out of plexiglass and contained 20 pressure taps on the roof surface and 16 pressure taps on the four walls to measure the external pressure distribution and a single pressure tap to measure the internal pressure.

The geometric and velocity scale ratios were 1/250 (λ_L) and 1/10 (λ_{Vel}), respectively. The internal volume of the model was scaled also to maintain similarity of the dynamic response of the volume at model scale to that in full scale. The internal volume scale (λ_{Vol}), as defined below, was calculated as follows:

$$\lambda_{Vol} = \frac{\lambda_L^{\,3}}{\lambda_{Vel}^{\,2}} = \frac{1}{156{,}250} \qquad (1)$$

In order to achieve this scale, a sealed volume chamber was installed at the bottom of the model so that its internal volume was increased proportionately based on the scaling law above.

Dominant openings and leakage through the building envelope were taken into consideration to evaluate the characteristics of internal pressure during the passage of a tornado with the building placed along the centerline of the tornado path. The building was oriented with its shorter wall normal to the translation direction of the tornado. Table 1 shows the geometry and opening ratio of dominant openings and leakage, where the opening ratio (r) is defined as the area of the opening to the total surface area of the building walls. Leakage in a real building will be distributed uniformly on the building envelope, comprising of walls and roof, and is a result of the porosity that naturally occurs in the building material.

3.2 Wind Pressure Measurement

High speed electronic pressure scanner (Scanivalve ZOC33/64Px) was used to measure the pressure distribution on the building model. Data were sampled for 24 seconds at the rate of 500Hz (12,000 data points). The initiation of data acquisition and the crane movement were synchronized using a common external trigger. The overall forces acting on the model were estimated by integrating the surface pressures. Wind pressure coefficients, as shown in the next section, were normalized using the respective maximum tangential velocity, $V_{\theta\max}$, and then ensemble averaged over 10 identical data runs.

3.3 Results of Wind Pressure Experiments

3.3.1 Characteristics of wind force on the roof (z-direction)

Figures 3 and 4 show the results of wind force coefficients in z direction as obtained from the pressure coefficients. Horizontal axis is the distance between the center of the tornado vortex and the center of the building model, x, normalized by the diameter of the tornado core, D.

(1) *Experimental cases where there are only leakages on walls* (*see Figure 3*)

Absolute value of external wind pressure coefficient, C_{pe}, increased as the simulator approached the model. It became maximum when x/D was ≈ ±0.5 and minimum when x/D was zero. In contrast, absolute value of internal wind pressure (suction) coefficient, C_{pi}, became maximum when x/D was zero where the maximum value increased with the opening ratio (r) of leakage which resulted in the maximum value of wind force coefficient, C_{Fz}, at x/D of ≈ ±0.5; these values were around 2.6 in the case of r=0.04% and around 1.8 in the case of r = 0.13%.

(2) *Experimental cases where there are leakages* (*r=0.13%*) *on walls and a dominant opening on*

one wall (*see Figure 4*)

In the experimental cases where there were not only distributed leakages but also a dominant opening on one wall, it was found that characteristics of the wind force on the roof depend on the location of the dominant opening. First, for the cases of dominant opening on wall #1 or #4, the value of C_{Fz} became maximum when x/D was ≈0.5, since the absolute value of C_{pi} was bigger when x/D was negative. In contrast, for the cases of dominant opening on wall #2 or #3 the characteristics of C_{Fz} showed different tendency from those above and it became maximum when x/D was ≈ −0.5. The internal pressure helped to reduce the peak uplift force on the roof significantly with a dominant opening present on wall # 1 or # 3 but not so much when the opening was on wall # 2 or # 4. The rotating wind enters the building through the opening on walls # 2 or # 4 and induces a positive internal pressure that reduces the magnitude of the internal pressure (suction) inside the building as induced by the static pressure drop inside the tornado core.

The value of C_{Fz} in each case discussed above was zero, when the center of vortex reached the center of model. The value of C_{pi} in each case had high correlation with the value of C_{pe} of the tap that was nearest to the dominant opening.

3.3.2 Characteristics of wind force on the wall (*x*- and *y*-direction)

Figure 5 shows the results of wind force coefficients in both *x* and *y* directions for the case where there are only distributed leakages (r=0.13%). As the tornado moves from the negative to the positive x direction, the value of C_{Fx} shows that the model was pulled first in the negative direction and then in the positive direction. The value of C_{Fy} follows the pattern of the tangential velocity component of the vortex. The tangential velocity exerted a positive C_{Fy} as the vortex first encountered the model, and then the value changed sign as the opposite side of the core passed over the model. The maximum of both C_{Fx} and C_{Fy} occurred very close to x/D = ±0.5 (i.e. at the radius of the vortex). This result is similar to those reported in Sengupta et al. (2008), where internal pressures were not considered, proving that internal pressure does not influence the overall loads on the walls that occur because of leakage.

4.0 PROBABILITY OF WIND-BORNE DEBRIS STRIKE

4.1 Experimental Setup

The low-rise building model and its orientation with respect to the tornado's translation axis, as used for the experiments discussed in this section of the paper, are the same as those of experiments discussed earlier in Section 3.1. Models of most commonly occurring wind-borne debris, i.e. 2 x 4 timber components, were made out of thick paper. Mass and reference area of the debris model were chosen to match those of the full scale based on Tachikawa number, *K*, as defined here:

$$K = \frac{\rho_a V^2 A}{2Mg} \tag{2}$$

where ρ_a is air density, V is tornado wind velocity, A is reference area, M is mass, and g is acceleration due to gravity, respectively, where velocity scale was calculated as 1/7. Table 2 shows the values of V, A, and M used here.

4.2 Method for Evaluation of the Strike Risk

For the case where the tornado approaches the building along its centerline, the probability of wind-borne debris striking the building walls was estimated in the following way. Figure 6 shows the number of each wall and location of potential wind-borne debris in normalized coordinates (x^*, y^*) as normalized by the radius of the vortex core, R .

Two hundred debris models were put at each location of potential wind-borne debris and then forced to scatter through the passage of the tornado simulator. By counting the number of the debris models which entered the model through the opening on the target wall (#*k*), the probability (p_k) of wind-borne debris striking the target wall #*k* were generated for each

location $(x^*, y^*) = (i, j)$, as follows:

$$p_k(i,j) = \frac{n_k}{n_0} \qquad (k = 1, \cdots, 4)$$
$$= \frac{1}{n_0} \cdot \left[\overline{N}_k(i,j) + \frac{t_\alpha}{\sqrt{3}} \cdot S_k(i,j) \right] \tag{3}$$

where n_0=200, $\overline{N}_k$ and S_k are mean and standard deviation of the sample number of debris models entering through the target opening in three trials, and t_α is 4.3 as listed in the Table of T distribution. Based on Equation (3) and the assumption that the strike of wind-borne debris on each wall are mutually independent, probability of wind-borne debris striking the building as a function of its location $(x^*, y^*) = (i, j)$, P, can be obtained by the following equation:

$$P(i,j) = \sum_{k=1}^{4} p_k(i,j) \tag{4}$$

4.3 Results of Experiment and Risk Evaluation

Figure 7 shows a snap shot of debris models flying around the building model and Figure 8 shows the probability of strike by wind-borne debris on each wall, p_k. The dark-gray filled circles in Figure 8 indicate the locations where the highest five probabilities were obtained.

Compared with the probability of strike on wall #2 or #4, probability corresponding to wall #1 was very small. This is because the direction of tangential wind velocity at y^*=0 is not perpendicular but parallel to that of wall #1. Strike probability corresponding to wall #3 was the same as that of wall #1. Strike probability corresponding to wall #2 or #4 increased with decrease in distance between potential location of debris generation and target building model. Moreover, while distribution of probabilities of strike on wall #4 was symmetric with respect to x^* axis, strike probabilities corresponding to wall #2 was not symmetric in the region of $-1 < x^*$. It is noted that probability was quite small in the region, defined by the dotted line $-1 < x^*$ and $0 < y^*$, because as the tornado simulator passes over the building model the debris models within the dotted region are picked up and thrown away from the model instead of striking wall # 2 which is located on the other side of this region.

Probabilities of debris strike based on Equation (4) are summarized in Figure 9. With respect to the potential debris locations in the region of $x^* <$ -1, all the probabilities shows a trend of inverse proportionality to the value of x^* raised to some power ($1/x^{*n}$). The power exponent (n) of x^* was calculated as 0.51 for $y^* = 0$, and 0.30 for $y^* = \pm 1$. In contrast, in the region of $-1 \leq x^* \leq 0$, probabilities for different y^* follows different trend from one another. While the value for $y^* =$ -1 is constant, approximately 0.45, the value for $y^* = 1$ had a gap at $x^* = -1$, which is seen in Figure 8(*b*). Further, the probability for $y^* = 0$, the value for $-1 < x^* < 0$ can be estimated by interpolating values between $x^* = -1$ and 0.

According to the results as discussed above, it is concluded that the characteristics of the risk of wind-borne debris strike on a building depends on whether or not the potential debris are located within a distance equivalent to the radius of tornado core from the center of the target building.

5.0 CONCLUSION

This paper summarizes the results of experimental studies related to wind hazards to low-rise buildings posed by tornadoes. The ISU tornado simulator at Iowa State University was used for these experiments. With respect to the results of wind pressure experiments, it was observed that the magnitude of internal pressure determines the total wind uplift force affecting the roof and that its characteristics depend on the magnitude of the distributed leakage and location of a dominant opening on the wall. Further, with respect to assessing risk of wind-borne debris strike, the experimental results show that the probability generally increases with decreasing distance between potential wind-borne debris and target building and the characteristics of the probability depends on whether the location of the potential debris is within or outside the region defined by one core radial distance of the tornado from the building center.

6.0 REFERENCES

Haan, F.L., Sarkar, P.P. and Gallus, W.A. (2008). "Design, Construction and Performance of a Large Tornado Simulator for Wind Engineering Applications." Engineering Structures, Vol. 30 (4), 1146-1159.

Oh, J.H., Kopp, G.A. and Inculet, D.R. (2007). "The UWO Contribution to the NIST Aerodynamic Database for Wind Load on Low Buildings: Part 3. Internal pressures." Journal of Wind Engineering and Industrial Aerodynamics, Vol. 95, 755-779.

Sengupta, A., Haan, F.L., Sarkar, P.P. and Balaramudu, V. (2008). "Transient Loads on Buildings in Microburst and Tornado Winds." Journal of Wind Engineering and Industrial Aerodynamics, Vol. 96 (10-11), 2173-2187.

Tachikawa, M. (1983). "Trajectories of Flat Plates in Uniform Flow with Application to Wind-Generated Missiles." Journal of Wind Engineering and Industrial Aerodynamics, Vol.14, 443-453.

Table 1: Geometry and ratio of dominant openings and leakage

Description of opening		Dimension (model scale)	Opening ratio, *r*
Distributed leakage	Two holes on each wall #1, 3	d=1.0mm	~0.04%
	Four holes on each wall #2, 4	d=1.8mm	~0.13%
Dominant opening		20.8mm x 7.6mm (wall #1, 3) 32.5mm x 7.6mm (wall #2, 4)	3.3%

Table 2: Parameters related to *V*, *A*, and *M*

	Full scale (*f*)	Model scale (*m*)
V	68m/s	9.7m/s
A	53cm x 10cm	3cm x 1.7cm
Mg	910g	0.2g

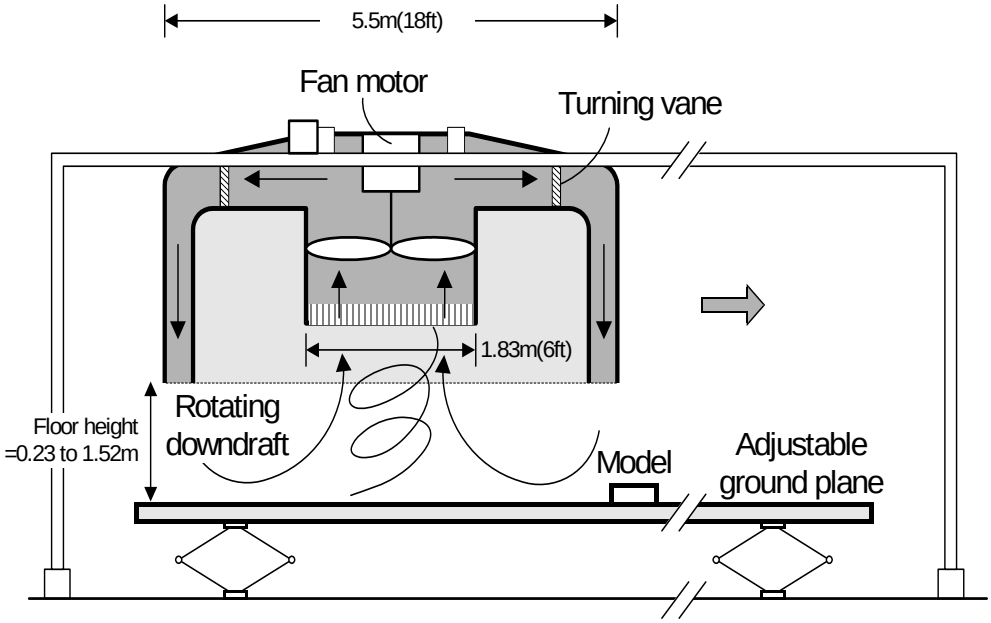

Figure 1: Schematic illustration of ISU Tornado Simulator

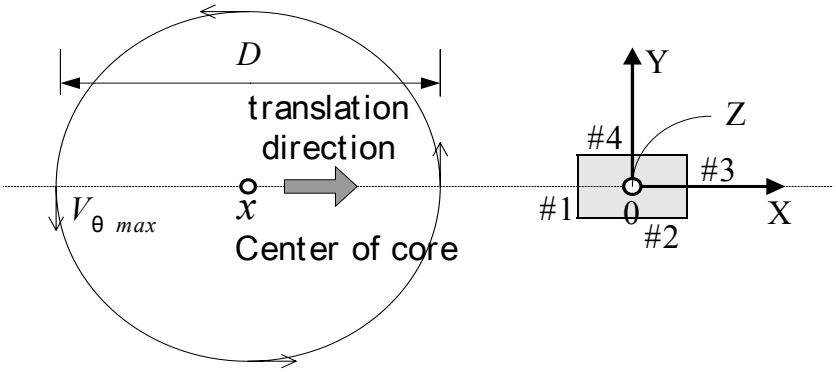

Figure 2: Definition of wall number and coordinates

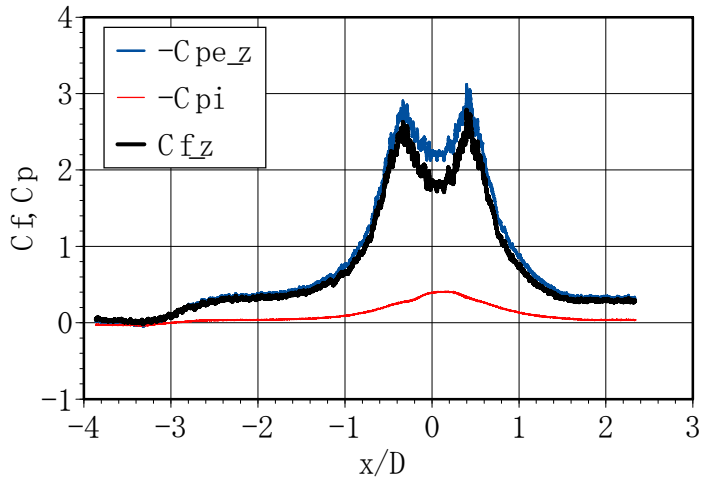

(*a*) r = ~0.04%

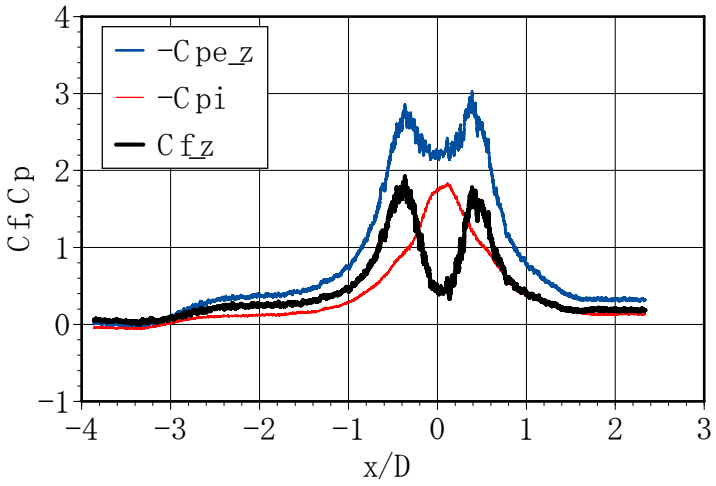

(*b*) r = ~0.13%

Figure 3: Wind Force Coefficients, C_{Fz} (Leakages Only)

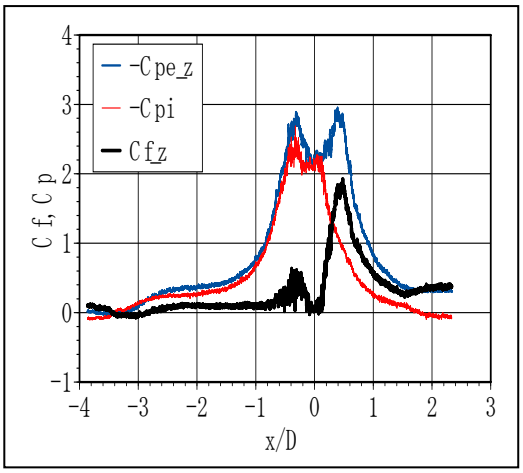

(*a*) Opening on Wall #1

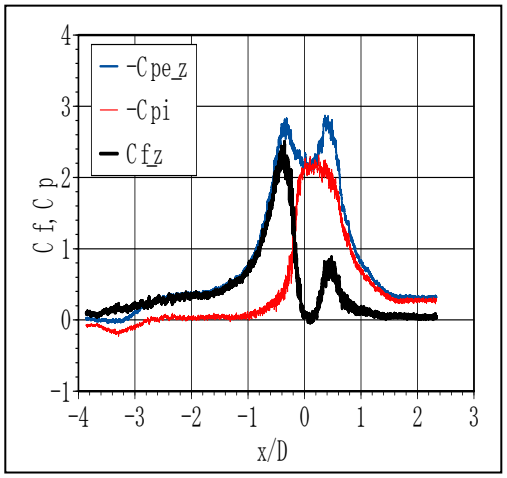

(*b*) Opening on Wall #2

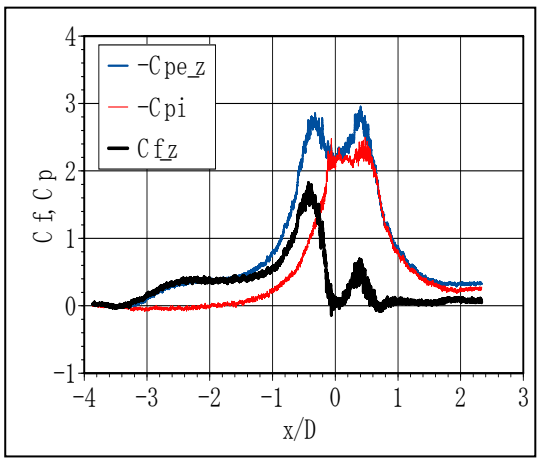

(*c*) Opening on Wall #3

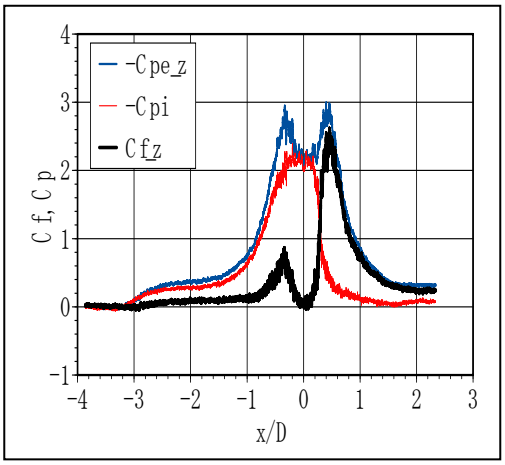

(*d*) Opening on Wall #4

Figure 4: Wind Force Coefficients, C_{Fz}, (Dominant Opening plus Leakage)

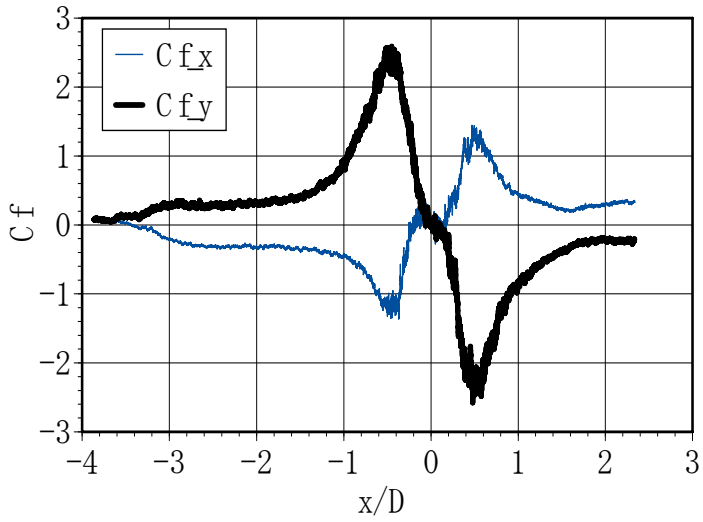

Figure 5: Wind Force Coefficients, C_{Fx}, C_{Fy}

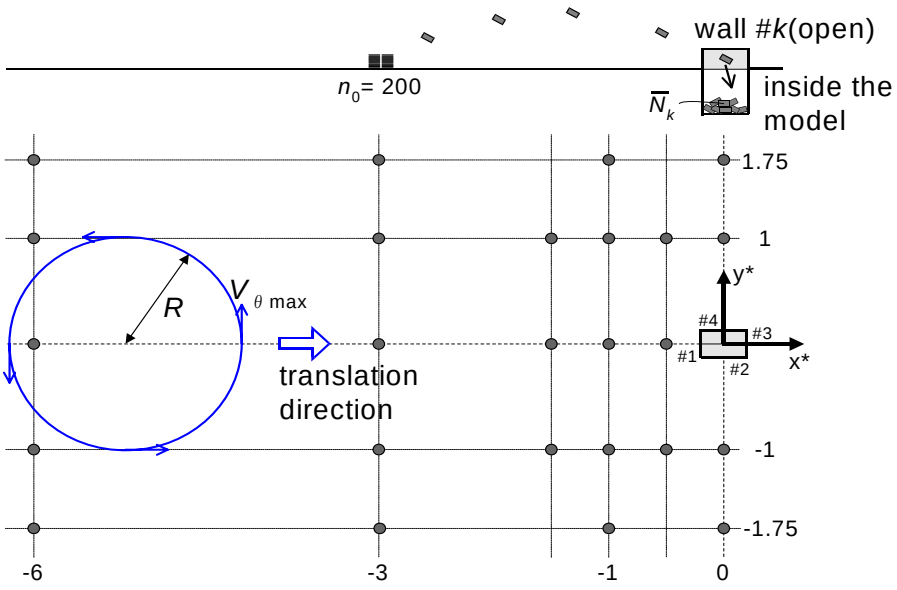

Figure 6: Definition of Wall Number, Coordinates, and Location of potential wind-borne debris in normalized coordinates ($x^*=x/R$, $y^*=y/R$) shown as dark dots.

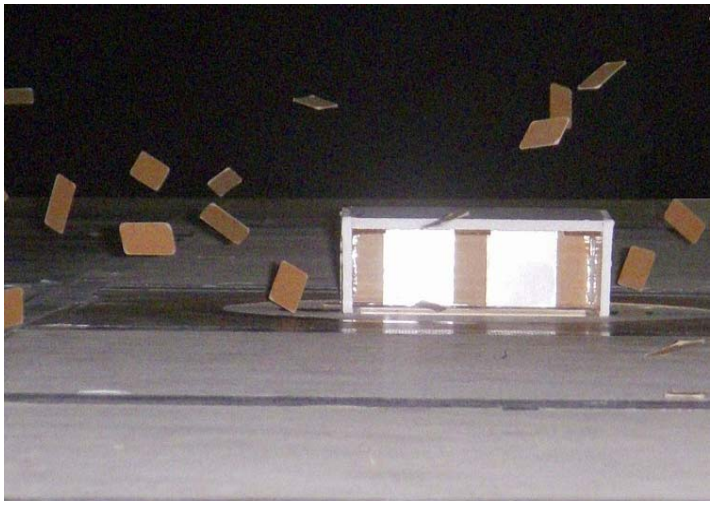

Figure 7: Debris models flying around building model

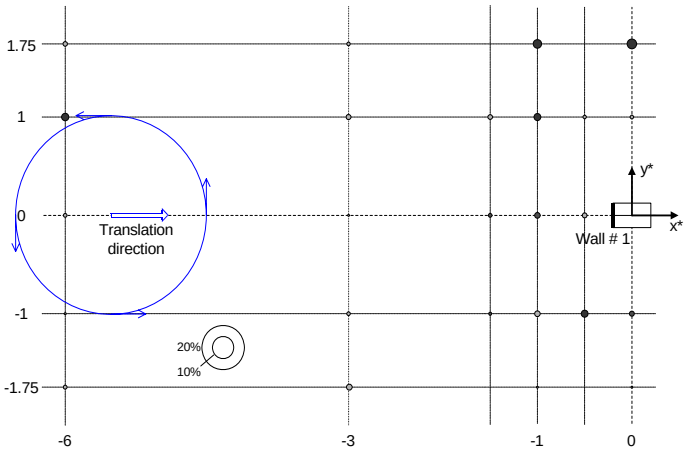

(*a*) Probability of Debris Strike on Wall #1, $p_1(i, j)$

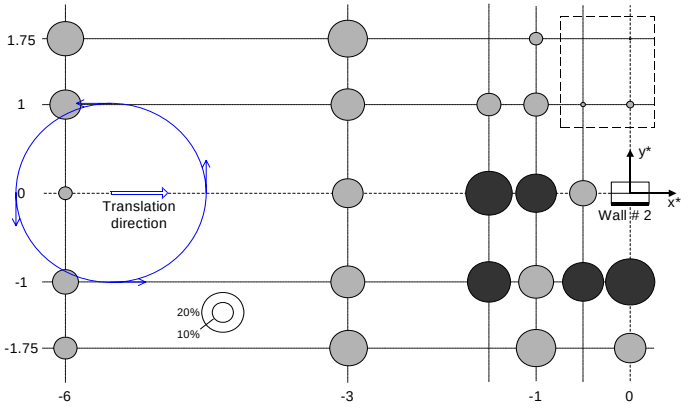

(*b*) Probability of Debris Strike on Wall #2, $p_2(i, j)$

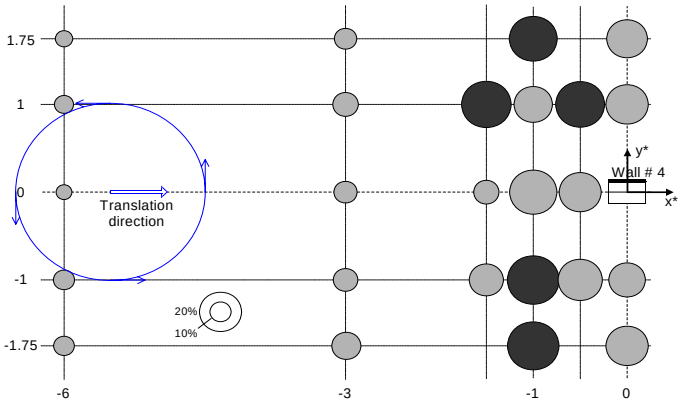

(*c*) Probability of Debris Strike on Wall #4, $p_4(i, j)$

Figure 8: Probability of debris strike on each wall

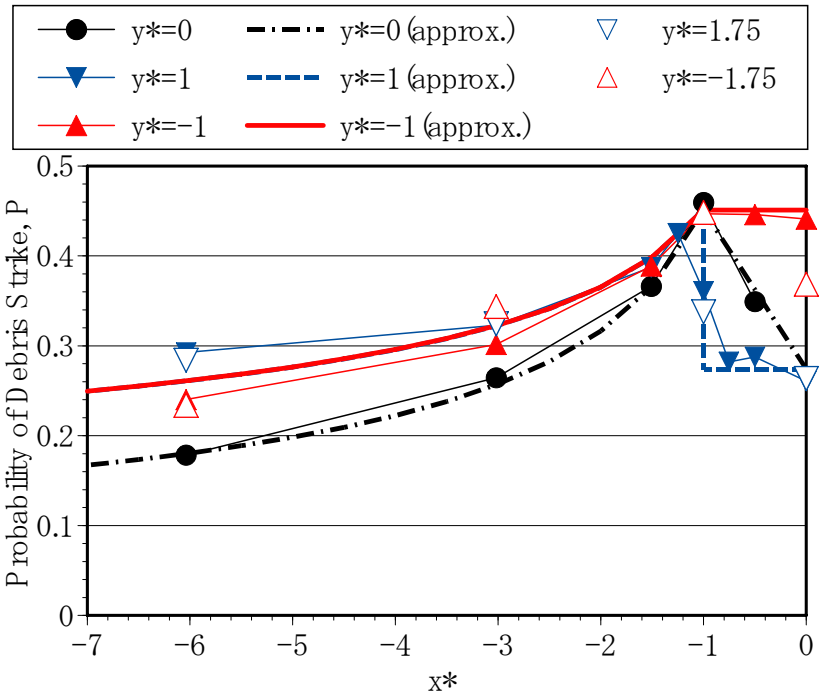

Figure 9: Probability of debris strike *vs*. Location of potential wind-borne debris